A novel technology to remove arsenic from drinking water for Bangladesh tubewells

Ashok Gadgil [1,2], Susan Addy [2], Case Van Genuchten [2]
1. Lawrence Berkeley National Laboratory, Berkeley, CA
2. Civil and Env. Engineering, University of California, Berkeley, CA

Presented at the AIChE 2010 Annual Meeting, Salt Lake City, UT: November 8, 2010

Abstract

Bangladesh and neighboring areas face large health threats from drinking arsenic-contaminated ground water. Arsenic levels in Bangladesh ground water are typically several hundred μg/L (compared to WHO recommendation of 10 μg/L for the MCL). About 50 million people drink such water, with hundreds of thousands already showing serious adverse health effects in what is described as the largest mass poisoning in history. The challenge is to develop a method for arsenic remediation that is (1) technically effective for removing arsenic down to 10 μg/L in the presence of other competing ions in the water, (2) affordable to most of the local population, (3) robust and easy to operate and maintain, and (4) does not require use of other toxic or hazardous chemicals. We describe a novel method that aims to meet these goals. ElectroChemical Arsenic Removal (ECAR) uses a small DC current and ordinary steel electrodes to produce a specific type of iron rust in the arsenic-contaminated ground water that binds to the arsenic and can be removed by filtration. We describe results using synthetic groundwater prepared in the laboratory, and also preliminary results from real Bangladesh groundwaters. We describe the design of a small ECAR reactor to treat 100 L of water at time, for a technical trial in West Bengal (India). Lastly, we show results from Extended X-ray Absorption Fine Structure (EXAFS) analysis that suggests the structure of the iron precipitate and the dominant mode of arsenic surface complexation.

1 Introduction

Arsenic contamination in groundwater has been discovered in Argentina, Chile, Mexico, China, Hungary, Vietnam, Cambodia, West Bengal (India), and Bangladesh [1, 2]. In most areas, surface waters are severely microbially contaminated, leaving no viable alternative drinking water source. In Bangladesh alone, 57 million people are exposed to arsenic levels of up to 3200 μg/L [3], well in excess of the maximum contaminant level (MCL) recommended by the World Health Organization of 10 μg/L [4]. A recent decade-long cohort study published in *The Lancet* found that 1 in 5 (21.3%) of all deaths in Bangladesh are attributable to arsenic in drinking water [5].

Arsenic exposure leads to dermatologic, neurologic, vascular, and carcinogenic effects [6]. It is known to cause skin, lung, bladder, urinary tract, and kidney cancer [7, 8]. Exposed children also suffer from a demonstrable decrease in intellectual function indicated by IQ [9, 10]. Increased health care and loss of productivity and income cost the average household as much as $84 per year [11] - a crippling burden on yearly income for those making US $1-2 per day.

Over twenty years after arsenic contamination was discovered in groundwater [12] no effective and affordable arsenic treatment technology has been implemented on a large scale [13-15]. Arsenic remediation units (ATUs) have failed to reach even 1% of the population at risk in Bangladesh [14]. The same is true for many safe water alternative methods such as

pond sand filters, rainwater harvesting, shrouded shallow dug wells, and piped water systems [14]. Lack of proper maintenance is consistently cited as a reason for ATU failure [13-17]. When ATUs are available and maintained, high upfront or ongoing costs prevent poor users from gaining access. The challenge is to develop a method for arsenic remediation that is (1) technically effective for removing arsenic down to 10 μg/L in the presence of other competing ions in the water, (2) affordable to most of the local population, (3) robust and easy to operate and maintain, and (4) does not require use of other toxic or hazardous chemicals.

ElectroChemical Arsenic Remediation (ECAR) is a form of Electrocoagulation (EC) that has been developed to meet the needs of an appropriate community scale implementation scheme that is financially viable, locally affordable, and offers long-term sustainable safe water access in rural areas [18, 19]. In ECAR, electrolytic oxidation of a sacrificial iron anode produces Hydrous Ferric Oxide (HFO; also called Fe(III) precipitates) in arsenic-contaminated water. Arsenic forms complexes with HFO, which then aggregate to form a floc that can be separated from water [20]. As(III) oxidation to As(V) occurs during the ECAR process [21, 22] either through electrolytic action at the electrode [21] or via highly reactive radical species produced by the oxidation of Fe(II) by dissolved oxygen [23, 24]. ECAR is promising due to many advantages over chemical coagulation - including pH buffering ability, ease of operation, amenability to automation, low maintenance, low sludge production, small system size, and the benefit of side reactions like electro-oxidation and electro-flotation [20, 21]. In ECAR, adsorbent media with a high capacity is generated during treatment, with no need for media regeneration or hazardous chemicals.

In this paper, we describe ECAR treatment results using arsenic-contaminated synthetic groundwater prepared in the laboratory, and also preliminary results from real groundwater in Bangladesh and Cambodia. We describe the design of a small ECAR reactor to treat 100 L of water at time, for a planned technical trial in West Bengal (India). Lastly, we show results from Extended X-ray Absorption Fine Structure (EXAFS) analysis that suggest the structure of the Iron precipitate and the dominant mode of Arsenic surface complexation.

2 ECAR Performance in Synthetic Groundwater

Arsenic removal is known to be highly sensitive to groundwater composition, specifically the presence of phosphate, silicate, natural iron and, to a lesser extent, carbonate, and calcium [24-26]. Each of these ions is present in contaminated Bangladesh groundwater [3]. Co-occurring Ions affect arsenic removal by competing with arsenic for sorption sites on HFO [24, 27], or by affecting the structure of HFO formed from Fe(II) oxidation [28, 29]. To understand ECAR arsenic removal performance in a relevant groundwater composition, batch tests were performed in Synthetic Bangladesh Groundwater (SBGW; Table 1) designed to mimic tubewell-water parameters in Bangladesh measured by BGS [3].

Table 1. Composition of Synthetic Bangladesh Groundwater (SBGW) for a representative initial total arsenic concentration of 600 μg/L .

Ion	Na^+ (mM)	Ca^{2+} (mM)	Mg^{2+} (mM)	Cl^- (mM)	HCO_3^- (mM)	SiO_3^{2-} (mM)	SO_4^{2-} (μM)	PO_4^{3-} (μM)	As(III) (μM)	As(V) (μM)	As(tot) μM	pH
SBGW	6.0	1.5	0.33	3.5	4.5	0.70	84	42	4.0	4.0	8.0	7.0

Batch experiments were performed in an electrochemical cell using an iron anode and copper electrode in arsenic-spiked SBGW, containing both As(III) and As(V). Contaminated

water was treated in 3-liter batches using a galvanostatic current. Treated solution was stirred for an additional 60 minutes with no electrodes. All tests were duplicated and the results averaged.

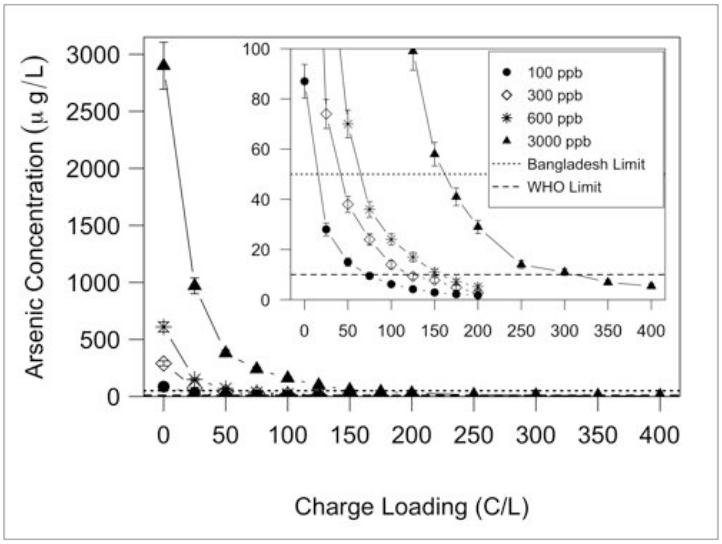

Figure 1. Aqueous arsenic concentration as a function of charge loading in Synthetic Bangladesh Groundwater (SBGW) for initial arsenic concentrations of 100 – 3000 μg/L (1:1 As(V):As(III)). Dotted and dashed lines indicate the legal Bangladesh limit (50 μg/L) and the WHO MCL (10 μg/L) respectively. Detail near the WHO MCL is shown in the inset.

Aqueous arsenic concentrations as a function of charge loading (i.e. the total charged passed through the electrochemical cell during electrolysis) for initial arsenic concentrations of 100 – 3000 μg/L are shown in Figure 1. In every case, ECAR reduces total arsenic in SBGW to well below the WHO MCL of 10 μg/L. The effect of initial concentration is to increase the charge loading required to reach the WHO MCL (see inset, Figure 1). Charge loading is directly related to the concentration of dissolved iron in solution by Faraday's law [30, 31], and thus can be thought of as a proxy for the HFO adsorbent dosage. An increase in the initial concentration is expected to require an increase in HFO adsorbent dosage to reach the WHO MCL.

It should be noted that numerous complicated processes are occurring simultaneously during ECAR, including the electrochemical dissolution of the electrode, Fe(II) oxidation and HFO hydrolysis, surface adsorption, and coagulation [20, 32]. ECAR operating parameters, such as the current density (current per active electrode area), charge loading, operating current, and post-electrolysis mixing time all have the potential to affect arsenic removal in subtle and sometimes complicated ways. It is beyond the scope of this paper to discuss or test the effect of each, though many have been explored to some extent in our lab [18].

3 Solid/Solution Separation

For robust and locally affordable operation in the field, a low cost method capable of separating arsenic-laden solids from water in a reasonable amount of time is needed. Low cost settling and decantation was compared to rapid but higher cost filtration using 0.1 μm filters after ECAR treatment in SBGW (Figure 2). Almost two days of settling was required for the former method to show solid separation comparable to filtering, or for the supernatant in

the settling solution to show acceptable (< 10 μg/L) arsenic levels. Variations in the required settling time were observed with different ECAR operating conditions, but > 1 day was always required. Significantly faster settling was observed when arsenic-spiked 0.1M NaCl solution was used in place of SBGW. Some ions found in groundwater are known to constrain precipitating HFO to small oligomers [29, 33, 34] which can be colloidally stable. X-ray Absorption Spectroscopy Spectra (discussed below) supports this hypothesis.

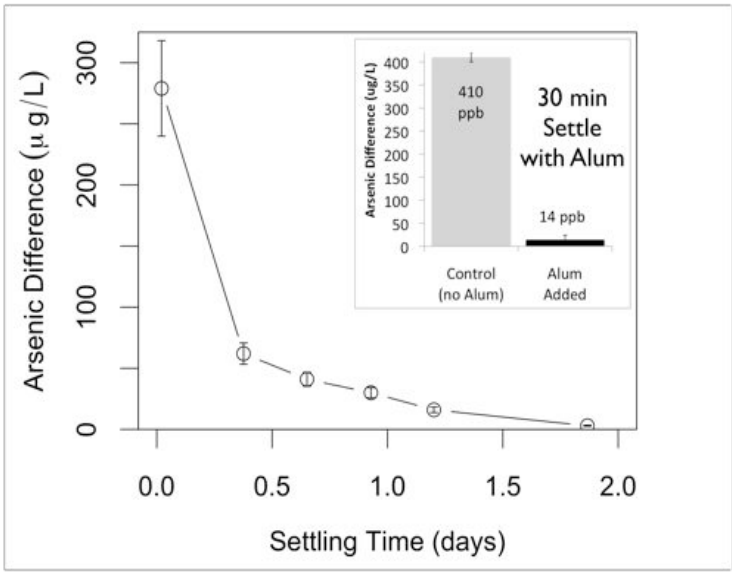

Figure 2. The difference in supernatant aqueous arsenic concentration between filtered (0.1 μm filters) and unfiltered samples while settling after ECAR treatment. The Inset shows data after 30 min of settling with and without 100 mg/L alum.

Addition of alum [$Al_2(SO_4)_3$ 18(H_2O)] solution as a coagulant significantly decreases the settling time of ECAR HFO particles in SBGW. Adding 100 mg/L alum immediately after electrolysis in combination with a 2 min rapid stir and a 25 min slow stir shows separation comparable to high cost filtration (see inset, Figure 2) after only 30 min of settling (57 min total with stir time). Subsequent tests showed that 25 mg/L alum is sufficient to achieve < 10 μg/L arsenic in the supernatant within 4 hours of settling (including stir time). Wholesale alum sells for about $0.08 - 0.24/kg [35], adding < 1% to the total operating costs.

4 ECAR Performance in Real Groundwater

4.1 Bangladesh

Six groundwater samples were obtained from arsenic contaminated tubewells in rural villages of Jhikargachha, Abhaynagar, and Sonargaon Upazilas in Bangladesh. One liter of water from each well was collected after approximately 5 minutes of pumping (to avoid bacterial contamination and oxygenated water in the well-head) and stored in tightly capped polyethylene bottles filled to the brim (for full sample collection and treatment procedures, see [18]).

Figure 3 shows the initial (immediately before treatment) and final (post-treatment) aqueous arsenic concentrations for Bangladesh groundwater samples treated with ECAR. In every case, ECAR is able to reduce initial arsenic concentrations of up to 510 μg/L to less than

the WHO MCL of 10 μg/L in real groundwater matrices. Samples BGS-1 to -4 were treated in the beaker scale setup described above. Samples BGW-5 and BGW-6, were treated in a bench-scale continuous flow prototype (described in [18]). One sample (BGW-7) was stored for 12 days and then filtered (no ECAR treatment) to determine the removal effect of naturally occurring iron precipitates in the tubewell water. Consistent with other passive sedimentation tests [24, 36], only a fraction of the arsenic was removed, and the final arsenic concentration (144 μg/L) was well above both the WHO MCL and the legal Bangladesh limit (50 μg/L).

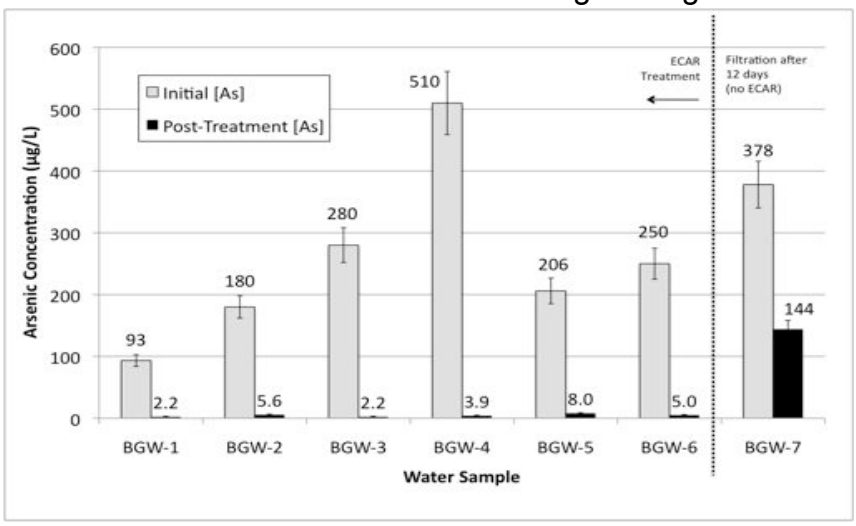

Figure 3. Arsenic concentration in samples collected from six tubewells in Bangladesh before (initial [As]) and after (Post-Treatment [As]) ECAR treatment. The rightmost bars show initial and post-treatment arsenic concentrations using passive sedimentation only (no ECAR treatment) after 12 days of sample storage.

4.2 Cambodia

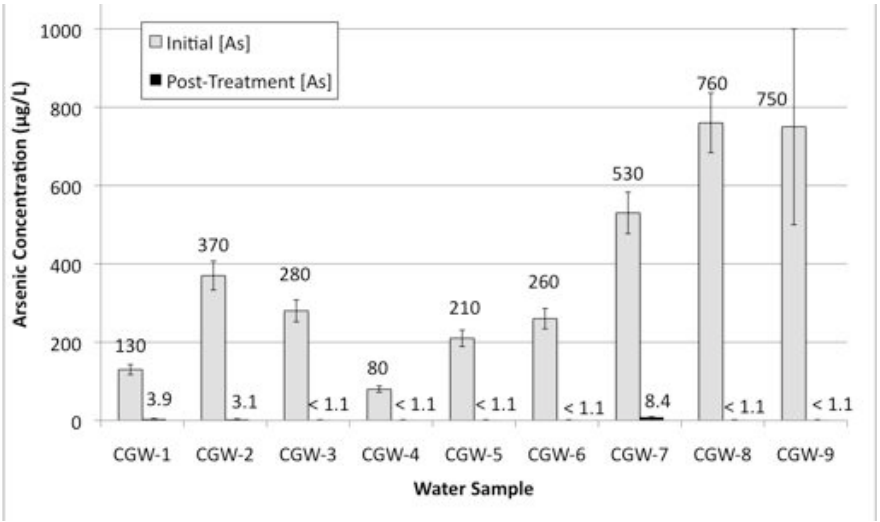

Figure 4. Arsenic concentration in samples collected from nine tubewells in Cambodia before (initial [As]) and after (Post-Treatment [As]) ECAR treatment.

Up to 1 million are at risk due to arsenic in drinking water in the Mekong Delta region of Cambodia and South Vietnam [2], primarily from aquifers with a different overall water composition than Bangladesh [25]. Nine arsenic-contaminated tube wells were chosen from the three communes Preak Russei, Dei Edth, and Preak Aeng in the Mekong Delta region of

Kandal Province, Cambodia (initial arsenic concentrations 80 – 750 μg/L). Arsenic concentrations before and after treatment with ECAR (using the bench-scale continuous flow prototype) are shown in Figure 4. In every case, ECAR-treated water contains less than 10 μg/L arsenic. In 6 of the 9 cases, final arsenic concentrations were below the detection limit of ICP-MS (< 1.1 μg/L).

5 Development and Performance of 100L Batch Prototype

A small 100L batch scale ECAR prototype has been designed, built, and tested in the lab for removing arsenic from SBGW. The prototype (Figure 5) comprises a cylindrical tank for dosing and mixing (Fig. 5a), connected to a sedimentation tank (Fig. 5b) for coagulant addition and solid/solution separation. The electrode assembly consists of 10 parallel mild steel plates (5 anode and 5 cathode) with alternate plates connected in series. The configuration allows for easy reversal of current, allowing each plate to alternate between anode and cathode to prevent extensive rust build up and passivation. A DC motor attached to a small impellor pushes water under the base plate and up between the electrode plates, allowing for efficient and even mixing between the plates.

a) b)

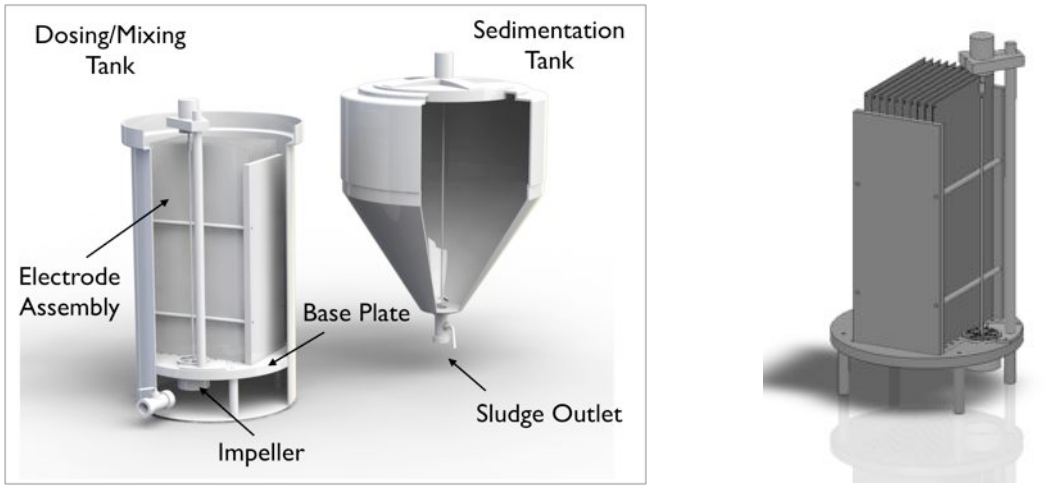

Figure 5. Cutaway rendering of (a) the full 100 L batch prototype (b) the electrode assembly and base plate only.

The prototype has successfully and repeatedly remediated SBGW with up to 3000 μg/L initial arsenic (with equal parts of As(III) and As(V)) to less than the WHO MCL in the lab, showing equal or better performance (in terms of required charge loading) than the bench-scale electrochemical cell. With the addition of a small amount of alum (25 mg/L), settling occurs within 4 hours, leaving a clear supernatant solution with < 10 μg/L arsenic. Sludge is easily accessed and collected through a valve at the cusp of the sedimentation tank. The amount of sludge collected per 100 L batch (including alum) is 10 – 20g for initial arsenic concentrations of 600 – 3000 μg/L. The prototype will be field tested in the highly arsenic-contaminated Murshidabad district of West Bengal, India, beginning in November of 2010.

6 Preliminary Results from XAS

X-ray absorption spectroscopy (XAS) is a powerful tool that allows for characterization of element-specific surface reactions on a molecular scale [37]. Fe K-Edge XAS spectra of arsenic-laden ECAR precipitates were collected to determine the predominate iron oxide

structure generated *in-situ* in SBGW, and to determine if any change in structure occurs when precipitates are generated at different current density, J (current per unit active electrode area). As K-Edge XAS spectra were collected to determine the predominant surface complex responsible for arsenic immobilization during the ECAR process.

Samples of arsenic-laden ECAR precipitates were collected after treating SBGW (initial arsenic concentration 600 μg/L) at current densities 0.02, 1.1, and 5.0 mA/cm^2. Solids were extracted using 0.1 μm filters and stored as a wet paste in a deoxygenated environment at 1ºC. Fe K-Edge XAS spectra were collected at beamline 10.3.2 of the Advanced Light Source (ALS) of Lawrence Berkeley National Laboratory (Berkeley, CA) at room temperature in transmission mode and calibrated using an Fe Foil. AsK-Edge XAS spectra were collected at beamline 11-2 of the Stanford Synchrotron Radiation Laboratory (SSRL; San Jose, CA) at room temperature in fluorescence and transmission mode and calibrated using an As Foil. Spectra were processed and analyzed using SixPack Software [38]. Full details of processing and analysis will be described elsewhere, but generally follow the procedures of [39]. A reference spectra for synthetic Geothite was provided by Dr. Brandy Toner; processing and analysis are similar to those described in [39].

Fourier transforms were performed over the k-range 3-11 Å^{-1} and 4-13.5 Å^{-1} for Fe and As respectively. By applying the Fourier transform to the $\chi(k)k^3$ data (where $\chi(k)$ is the Extended X-ray Absorption Fine Structure, or EXAFS, spectra), it is possible to extract individual frequencies that contribute to the overall data and convert them to peaks resembling a radial distribution function (RDF). These peaks are related to the interatomic distance between the absorbing atom and its nearest neighbors but vary by a *phase shift,* ΔR, resulting in a peak shift of approximately -0.3 to -0.5 Å depending on the type of interacting atoms.

6.1.1 Iron Shell-by-shell fits

The Fourier transformed Fe data for ECAR precipitates prepared at current densities J = 0.02, 1.1, and 5.0 mA/cm^2 are compared to that of Goethite in Figure 6a. The first peak represents the first shell (Fe-O) bonds within the FeO_6 octahedra, and is shared between the ECAR samples and Goethite. The best theoretical curve fit to ECAR samples (overlaid in Figure 6a) indicates two distinct Fe-O distances at 1.93 and 2.04 Å, suggesting a small, but significant distortion of the FeO_6 octahedra. These distances are in agreement with EXAFS measurements of FeO_6 octahedra in amorphous and crystalline iron phases [33, 34, 39].

The second shell of iron (oxyhydr)oxides is typically due to Fe-Fe pairs and contains more meaningful structural information. Here there is a clear difference between the ECAR samples and Goethite (Figure 6a). In the polyhedral approach, the polymerization of individual FeO_6 octahedra into crystalline iron phases occurs by corner-, edge-, and face- sharing octahedral linkages [40, 41]. These different topologies have characteristic Fe-Fe interatomic distances (indicated by a vertical line in Figure 6a) that can be distinguished in the second shell peak. Theoretical curve fitting showed that, although multiple Fe-Fe paths are seen in the fit of goethite, only one Fe-Fe path at approximately 3.06 Å was required for the best fit of EC precipitates. The spatial resolution, given by $\pi/2\Delta k$ where Δk is the k-range of the data used in transform [42, 43], is 0.2 Å. This is sufficient to resolve second-shell contributions from paths at 3.23 and 3.43 Å. Forcing additional Fe-Fe paths with these distances into the fit yielded physically impossible N_{Fe-Fe} (coordination number) values and excessive (and often

negative) values of σ^2 (mean squared displacement parameter). This suggests that FeO_6 octahedra joined by corner-sharing linkages were not present in detectable amounts. Further confirmation is provided by the lack of a characteristic beat-node in the back-transformation of the second shell peak for ECAR precipitates (data not shown).

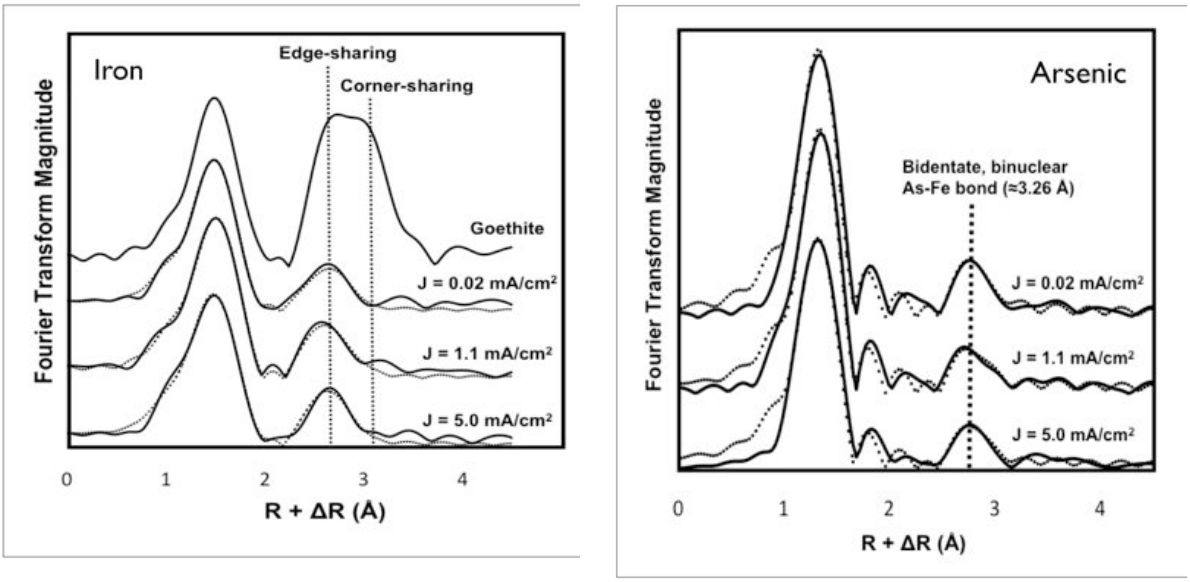

Figure 6. (a) Fe- and (b) As-K-Edge Fourier transform magnitude uncorrected for phase shift, for Goethite (Fe only) and ECAR particulates generated at current densities J = 0.02, 1.1, and 5.0 mA/cm^2 (data = solid, shell-by-shell fits = dotted).

The absence of any corner-sharing octahedra can be explained by the ions present in SBGW. Amorphous iron phases similar to EC precipitates exhibit strong affinities for sorption of SiO_3^{2-}, PO_4^{3-}, and AsO_4^{3-} [44], all present in SBGW (Table 1). These oxyanions sorb strongly onto the growth site where FeO_6 octahedra would form double corner-sharing linkages [33, 34, 45, 46] a phenomenon known as surface poisoning. The result of surface poisoning is a 2-dimensional cluster of edge-sharing FeO_6 octahedra with SiO_3^{2-}, PO_4^{3-}, and AsO_4^{3-} bound by corner sharing with adjacent FeO_6 octahedra. Nanoparticulate iron oxides have very high surface area to volume ratios, which leads to enhanced contaminant sorption per adsorbent mass. However, the bound oxyanions also help generate colloidally stable FeO_6 clusters that are difficult to separate from solution. This is likely the cause of the long (2 day) settling times observed for ECAR particles (Figure 2).

6.1.2 Arsenic Shell-by-Shell Fits

First shell As-O fits (Figure 6b) for all ECAR samples are consistent with previous studies of tetrahedrally coordinated As(V) sorbed to iron (oxyhydr)oxides [47, 48], supporting As(III) oxidation to As(V) during the EC process. As(III) oxidation is also supported by the XANES (X-ray Absorption Near Edge Spectra) structure (data not shown).

Similar to Fe analysis, the second peak of the transformed As data is the most important to properly characterize the structure of bound As. If the surface complex is inner-sphere, three possible geometries exist: (1) bidentate, mononuclear (^{2}E) complexes that share edges between AsO_4 and FeO_6 polyhedra (As-Fe distance ~ 2.8-2.9 Å), (2) AsO_4 tetrahedra bound in bidentate, binuclear complexes (^{2}C) that bridge oxygen atoms of adjacent FeO_6 octahedra (As-Fe distance ~ 3.2-3.3 Å), and (3) monodentate, mononuclear (^{1}C) complexes

that share single corners between AsO_4 and FeO_6 polyhedra (As-Fe distance ~ 3.5-3.6 Å) [49]. If As is present as an outer-sphere complex, there would be a contribution to the signal above 4 Å, which does not appear in our data. The results of theoretical curve fitting suggest that the ^2C configuration is the primary geometry seen in the data. The data did not support the presence of a large fraction of the ^2E and ^1C geometries, and did not support the formation of AsO_4 polymers.

Due to the nanoscale nature of the EC precipitates suggested by shell-by-shell fits of the Fe k-edge peaks, the reduced contribution of the ^2E geometry is somewhat surprising. Short-ranged polymers consisting of only small clusters of edge-sharing FeO_6 octahedra should exhibit maximized edge-sharing sites [50]. The lack of support for this geometry may be due to the higher surface free energy of the ^2E geometry suggested by [51].

6.1.3 Effect of Current Density

The Fourier transformed spectra for Fe and As (Figure 6) shows little to no change across current densities J = 0.02 – 5.0 mA/cm^2, indicating that both the predominate iron oxide structure of precipitates and predominant arsenic surface complex are likely the same within this range. Shell-by-shell fits confirm that best fit parameters are consistent between samples for both Fe and As. This suggests that it is not possible to tune the iron oxide structure for improved As-adsorption by adjusting the current density within the tested range. However, it also suggests that the arsenic adsorption capacity of EC precipitates will be similar across current densities, allowing adjustment of the current density parameter to focus on other goals, such as short treatment-time or low power consumption.

7 Conclusions

Electrochemical arsenic remediation (ECAR) has been successfully tested in synthetic Bangladesh water and found capable of mitigating initial arsenic (including As(III)) from up to 3000 μg/L to below the WHO MCL of 10 μg/L. Separation by low-cost sedimentation can occur in <4 hours with the addition of 25 mg/L alum. ECAR treatment has been demonstrated to successfully mitigate real Bangladesh groundwater (initial arsenic 93 – 510 μg/L) and real Cambodia groundwater ((initial arsenic 80 – 760 μg/L). In all cases, ECAR was able to reduce arsenic levels to below the WHO MCL of 10 μg/L. A small-scale batch 100 L prototype has been fabricated and successfully tested in the lab using synthetic Bangladesh groundwater. It will be field tested in West Bengal, India in November 2010.

Shell-by-shell fits to Fe K-Edge XAS spectra showed only edge linkages and did not support corner linkages, likely caused by SiO_3^{2-}, PO_4^{3-}, and AsO_4^{3-} ions sorbing to corner linkage sites. This constrains HFO generated in ECAR to stable colloidal particles, explaining the long observed settling time when no coagulants are added. As K-Edge spectra fits suggest arsenic is bound to HFO by strong bidentate, binuclear complexes. Changing the current density of ECAR operation within a range of J = 0.02 to 5.0 mA/cm^2 caused no change in the generated HFO structure or arsenic complexes formed.

Acknowledgements

We gratefully acknowledge support for this work by The Richard C. Blum Center for Developing Economies, a USEPA P3 Phase II award, The Sustainable Products and Solutions Program at Haas School of Business at UC Berkeley, an award from the UC Berkeley Bears

Breaking Boundaries Contest, and Jane Lewis Fellowship support to one of the authors (CVG). We are also thankful to Iqbal and Kamal Quadir, the CE290 Spring 2007 BEAR team, the many current and past student-members of BAAG, and particularly to Mathew Marcus, Sirine Fakra, John Bargar, Jackie Pena, Brandy Toner, Jonathan Slack, and Howdy Goudey.

References

1. Petrusevski, B., et al., *Arsenic in Drinking Water*, 2007, IRC International Water and Sanitation Centre, Thematic Overview Paper 17: Netherlands.
2. Berg, M., et al., *Magnitude of arsenic pollution in the Mekong and Red River Deltas--Cambodia and Vietnam.* Science of the Total Environment, 2007. **372**(2-3): p. 413-425.
3. BGS, *Arsenic Contamination of Groundwater in Bangladesh*, D.G. Kinniburgh and P.L. Smedley, Editors. 2001, WC/00/19, British Geological Survey: Keyworth, U.K.
4. WHO, *Guidlines for Drinking-Water Quality*, 1993, The World Health Organization: Geneva, Switzerland.
5. Argos, M., et al., *Arsenic exposure from drinking water, and all-cause and chronic-disease mortalities in Bangladesh (HEALS): a prospective cohort study.* The Lancet, 2010. **10**: p. 60481-60483.
6. Chowdhury, U.K., et al., *Groundwater Arsenic Contamination in Bangladesh and West Bengal, India.* Environmental Health Perspectives, 2000. **108**(5): p. 393-397.
7. Tchounwou, P., A. Patlolla, and J. Centeno, *Carcinogenic and systemic health effects associated with arsenic exposure - A critical review.* Toxicologic Pathology, 2003. **31**(6): p. 575-588.
8. Abernathy, C., D. Thomas, and R. Calderon, *Health effects and risk assessment of arsenic.* Journal of Nutrition, 2003. **133**(5, Suppl. 1): p. 1536S-1538S.
9. Wasserman, G.A., et al., *Water Arsenic Exposure and Children's Intellectual Function in Araihazar, Bangladesh.* Environmental Health Perspectives, 2004. **112**(13): p. 1329-1333.
10. Wang, S.X., et al., *Arsenic and fluoride exposure in drinking water: Children's IQ and growth in Shanyin county, Shanxi province, China.* Environmental Health Perspectives, 2007. **115**(4): p. 643-647.
11. Roy, J., *Economic benefits of arsenic removal from ground water -- A case study from West Bengal, India.* Science of the Total Environment, 2008. **397**(1-3): p. 1-12.
12. Garai, R., et al., *Chronic arsenic poisoning from tube-well water.* Journal of the Indian Medical Association, 1984. **82**(1): p. 34-35.
13. Kabir, A. and G. Howard, *Sustainability of arsenic mitigation in Bangladesh: Results of a functionality survey.* International Journal of Environmental Health Research, 2007. **17**(3): p. 207-218.
14. Ahmed, M., et al., *Ensuring safe drinking water in Bangladesh.* Science, 2006. **314**(5806): p. 1687-1688.
15. Hossain, M.A., et al., *Ineffectiveness and Poor Reliability of Arsenic Removal Plants in West Bengal, India.* Environmental Science and Technology, 2005. **39**(11): p. 4300-4306.
16. Hoque, B.A., et al., *Demand-based water options for arsenic mitigation: an experience from rural Bangladesh.* Public Health, 2004. **118**(1): p. 70-7.
17. Ahmad, J., et al., *Willingness to Pay for Arsenic-Free, Safe Drinking Water in Bangladesh*, 2003, Water and Sanitation Programme--South Asia, The World Bank: New Delhi, India.

18. Addy, S.E.A., *Electrochemical Arsenic Remediation for Rural Bangladesh, PhD Thesis*, 2008, University of California - Berkeley. Available at: http://repositories.cdlib.org/lbnl/LBNL-1405E/.
19. Addy, S.E.A., et al., *Electrochemical Arsenic Remediation for Rural Bangladesh*, in *Proceedings of the Symposium on Sustainable and Safe Drinking Water in Developing and Developed Countries: Where Science Meets Policy,* 2008: Chapel Hill, NC. Available at: http://www.escholarship.org/uc/item/7bp8p38b.
20. Mollah, M.Y.A., et al., *Fundamentals, present and future perspectives of electrocoagulation.* Journal of Hazardous Materials, 2004. **114**(1-3): p. 199-210.
21. Kumar, P.R., et al., *Removal of arsenic from water by electrocoagulation.* Chemosphere, 2004. **55**(9): p. 1245-1252.
22. Wan, W., et al., *Effects of water chemistry on arsenic removal from drinking water by electrocoagulation.* Water Research, 2010. **in press**.
23. Hug, S.J. and O. Leupin, *Iron-Catalyzed Oxidation of Arsenic(III) by Oxygen and by Hydrogen Peroxide; pH-Dependent Formation of Oxidants in the Fenton Reaction.* Environmental Science and Technology, 2003. **37**(12): p. 2734-2742.
24. Roberts, L.C., et al., *Arsenic Removal with Iron(II) and Iron(III) in Waters with High Silicate and Phosphate Concentrations.* Environmental Science and Technology, 2004. **38**(1): p. 307-315.
25. Hug, S.J., O.X. Leupin, and M. Berg, *Bangladesh and Vietnam: Different groundwater compositions require different approaches to arsenic mitigation.* Environmental Science and Technology, 2008. **42**(17): p. 6318-6323.
26. Guan, X., et al., *Removal of arsenic from water: Effect of calcium ions on As(III) removal in the KMnO4–Fe(II) process.* Water Research, 2009. **43**(20): p. 5119-5128.
27. Meng, X.G., et al., *Combined effects of anions on arsenic removal by iron hydroxides.* Toxicology Letters, 2002. **133**(1): p. 103-111.
28. Ahmad, J., S. Misra, and B. Goldar, *Rural communities' preferences for arsenic mitigation options in Bangladesh.* Journal of water and health, 2006. **4**(4): p. 463.
29. Voegelin, A., et al., *Effect of phosphate, silicate, and Ca on Fe(III)-precipitates formed in aerated Fe(II)- and As(III)-containing water studied by X-ray absorption spectroscopy.* Geochimica Et Cosmochimica Acta, 2010. **74**(1): p. 164-186.
30. Gu, Z., et al., *Estimating Dosing Rates and Energy Consumption for Electrocoagulation Using Iron and Aluminum Electrodes.* Industrial and Engineering Chemistry Research, 2009. **48**(6): p. 3112-3117.
31. Lakshmanan, D., D.A. Clifford, and G. Samanta, *Ferrous and Ferric Ion Generation During Electrocoagulation.* Environmental Science and Technology, 2009. **43**: p. 3853-3859.
32. Holt, P.K., Barton G.W. Mitchell C.A., *The future for electrocoagulation as a localised water treatment technology.* Chemosphere, 2005. **59**(3): p. 355-367.
33. Doelsch, E., et al., *Speciation and crystal chemistry of Fe(III) chloride hydrolyzed in the presence of SiO4 ligands. 2. Characterization of Si-Fe aggregates by FTIR and Si-29 solid-state NMR.* Langmuir, 2001. **17**(5): p. 1399-1405.
34. Rose, J., et al., *Nucleation and growth mechanisms of Fe oxyhydroxide in the presence of PO4 ions. 1. Fe K-edge EXAFS study.* Langmuir, 1996. **12**(26): p. 6701-6707.
35. Jiang, F., et al., *Estimation of costs of phosphorous removal in wastewater treatment facilities: Adaptation of existing facilities* 2005, Georgia Water Planning and Policy Center, Andrew Young School of Policy Studies, Georgia State University, Atlanta.

36. WaterAid, *Rapid Assessment of Household Level Arsenic Removal Technologies. Phase I--Final Draft Report*, 2001, BAMWSP/DFID/WaterAid.
37. Norman, D., *X-ray absorption spectroscopy (EXAFS and XANES) at surfaces* Journal of Physics C-Solid State Physics, 1986. **19**(18): p. 3273-3311.
38. Webb, S.M., *SIXPack: A graphical interface for XAS analysis using IFFEFFIT presented by Samuel Webb.* Physica Scripta, 2003. **T115**.
39. Toner, B.M., et al., *Biogenic iron oxyhydroxide formation at mid-ocean ridge hydrothermal vents: Juan de Fuca Ridge.* Geochimica et Cosmochimica Acta, 2009. **73**(2): p. 388-403.
40. Manceau, A. and J.M. Combes, *Structure of Mn and Fe Oxides and Oxyhydroxides - A Topical Approach by EXAFS.* Physics and Chemistry of Minerals, 1988. **15**(3): p. 283-295.
41. Combes, J.M., et al., *Formation of ferric oxides from aqueous solutions: A polyhedral approach by X-ray absorption spectroscopy: I. Hydrolysis and formation of ferric gels.* Geochimica Et Cosmochimica Acta, 1989. **53**(3): p. 583-594.
42. Bunker, G., *Introduction to EXAFS : a practical guide to X-ray absorption fine structure spectroscopy.* 2010, Cambridge, UK; New York: Cambridge University Press.
43. Ulery, A.L. and L.R. Drees, *Methods of soil analysis. Part 5, Mineralogical methods*2008, Madison, WI: Soil Science Society of America.
44. Leupin, O.X. and S.J. Hug, *Oxidation and removal of arsenic (III) from aerated groundwater by filtration through sand and zero-valent iron.* Water Research, 2005. **39**(9): p. 1729-1740.
45. Waychunas, G.A., et al., *Surface Chemistry of Ferrihydrite. 1. EXAFS Studies of the Geometry of Coprecipitated and Adsorbed Arsenate.* Geochimica Et Cosmochimica Acta, 1993. **57**(10): p. 2251-2269.
46. Rose, J., et al., *Nucleation and Growth Mechanisms of Fe Oxyhydroxide in the Presence of PO4 Ions. 2. P K-Edge EXAFS Study.* Langmuir, 1997. **13**(6): p. 1827-1834.
47. Morin, G., et al., *Extended X-ray absorption fine structure analysis of arsenite and arsenate adsorption on maghemite.* Environmental Science and Technology, 2008. **42**: p. 2361-2366.
48. Manning, B.A., et al., *Arsenic(III) and Arsenic(V) reactions with zerovalent iron corrosion products.* Environmental Science and Technology, 2002. **36**(24): p. 5455-5461.
49. Ona-Nguema, G., et al., *EXAFS analysis of arsenite adsorption onto two-line ferrihydrite, hematite, goethite, and lepidocrocite.* Environmental Science and Technology, 2005. **39**(23): p. 9147-9155.
50. Waychunas, G.A., J.A. Davis, and C.C. Fuller, *Geomety of Sorbed Arsenate on Ferrihydrite and Crystalline FeOOH - Reevaluation of EXAFS results and Topological Factors in Predicting Sorbate Geometry, and Evidence for Monodentate Complexes.* Geochimica Et Cosmochimica Acta, 1995. **59**(17): p. 3655-3661.
51. Sherman, D.M. and S.R. Randall, *Surface complexation of arsenic(V) to iron(III) (hydr)oxides: structural mechanism from ab initio molecular geometries and EXAFS spectroscopy.* Geochimica Et Cosmochimica Acta, 2003. **67**(22): p. 4223-4230.